Journal of Ceramic Processing Research. Vol. 1, No. 1, pp. 74~79 (2000)

J O U R N A L O F
Ceramic Processing Research

Computer aided design of electric insulator

Y.T. Keum*, J.H. Kim* and B.Y. Ghoo[a]
CPRC, Hanyang University, Seoul, Korea
[a]Graduate School, Hanyang University

For the optimal design of a ceramic electric insulator, the drying and structural analyses are performed. The heat and moisture movements in green ceramics caused by the interaction of temperature gradient, moisture gradient, conduction, convection, and evaporation are considered in the hygro-thermal analysis. The finite element method for solving the temperature and moisture distributions, which not only change the volume but also induce the stress, is employed. Also, the structural analysis of the ceramic insulator supporting the electric cable weight is carried out using a finite element code, in which axi-symmetric structural and interface elements describe the material behavior to external loads. Based on the drying and structural analyses, the guidelines of precise design of ceramic insulators were prepared and the new geometry of ceramic insulator was proposed by virtue of computer aided design.

Key words: Finite element simulation, Ceramic drying analysis, Ceramic structural analysis, Ceramic electric insulator, Computer aided design.

Introduction

Since the design of ceramic products has to consider the outward appearance, strength, deformation, residual stress, and fracture toughness etc., their quantitative evaluation is essential for a proper design. Unfortunately, it cannot be easily done because most ceramic products involve cranky drying processes. Furthermore, it has been dependant on the know-how technique of design engineers. Recently, the computer aided numerical methods like FEM, FDM, and BEM are widely used to evaluate the mechanical characteristics as well as to optimize the design of ceramic products. Using numerical methods, the mechanical characteristics of ceramics affected by the temperature, moisture, and loads can be easily evaluated.

The variations of temperature and moisture caused by the heat and moisture transfer in the drying process not only change the volume but also induce the hygro-thermal stress. The heat and moisture transfer and the associated hygro-thermal stress are the fundamental issue in heat-moisture-stress problems. To find quantitatively the temperature profile, moisture distribution, deformation, and residual stresses of the ceramic during the drying process, FEM simulation is a favorable method because the experimental evaluation is not technically proper and the numerical model is not geometrically simple.

As the crack and fracture of ceramics are occurred by various loading conditions such as the static load, dynamic load, fatigue load etc., they need to be considered in a design stage to avoid such problems. A failure by the loading conditions can be detected by the structural analysis.

The interrelation between heat and moisture transfer in porous materials was established by Luikov [1-3] who proposed two terms relationship for a non-isothermal moisture diffusion. The development of the theory of transport phenomena in porous media has been summarized by Luikov and Whitaker [4]. Later, Luikov [2, 3] noticed the similarity between the relation of enthalpy with temperature and the relation of moisture content with the moisture potential. Also, the effects of the liquid and vapor transport, heat transport, pressure gradient, and capillary flow were investigated by De Vries *et al.* [5, 6] and a set of coupled diffusion equations of temperature and moisture contents were proposed. Whitaker [4] analyzed the heat, mass, and momentum in porous media and Comini *et al.* [7] performed the numerical analysis of the two-dimensional problem involving heat and mass transfer. The validity of this methodology in timber was verified through the comparison between experimental and numerical results by Thomas *et al.* [8] Stress distribution caused by heat and moisture transfer was analyzed by Lewis *et al.* [11] using the finite element method in the drying process of a brick, a ceramic electric insulator, and a foundation basement. The hygro-thermal stress caused by heat and moisture transfer in composite materials was also analyzed by Sih *et al.* [12] Heuer [13] simulated a structural analysis for a cone-shaped insulator with ANSYS and Iwama and

*Corresponding author:
Tel : 02-2290-0436
Fax: 02-2294-6194
E-mail: ytkeum@email.hanyang.ac.kr

Kito [14] compared the stress distribution obtained from simulations with that found by empirical equations.

In this study, the finite element simulation of ceramic electric insulators was performed for analyzing the heat and moisture transfer in the drying process and overloading conditions in suspending cable weight. The guideline of precise design of ceramic insulators is proposed on the basis of computer simulations and the redesign of the insulator geometry is introduced.

Finite Element Formulation

Drying Analysis

The coupled diffusion equations for temperature and moisture transfer are derived using the framework presented by Luikov [1-3]. Namely,

$$C\frac{\partial T}{\partial t} = -\nabla \cdot \boldsymbol{j}_q + \dot{I}_q = \nabla \cdot (\boldsymbol{K}^M \cdot \nabla W + \boldsymbol{K}^T \cdot \nabla T) + \dot{I}_q \tag{1}$$

$$\frac{\partial W}{\partial t} = -\nabla \cdot \boldsymbol{j}_m = \nabla \cdot (\boldsymbol{A}^M \cdot \nabla W + \boldsymbol{A}^T \cdot \nabla T + \boldsymbol{A}^g \cdot Wg) \tag{2}$$

where T is temperature, W is the moisture, C is the bulk specific heat per unit volume, $\boldsymbol{j}_q$ is the heat flux vector, $\boldsymbol{j}_m$ is the moisture flux vector, i_q is the heat source function, $\boldsymbol{K}^M$ is the diffusion-thermal coefficient tensor, $\boldsymbol{K}^T$ is the heat conductivity tensor, $\boldsymbol{A}^M$ is the moisture diffusivity tensor, $\boldsymbol{A}^T$ is the thermal diffusion coefficient tensor, and $\boldsymbol{A}^g$ is the forced flux coefficient tensor. Also, the boundary conditions are given as follows (see Fig. 1):

$$T = Ta \text{ on } S_1 \tag{3}$$

$$k_q \nabla T\boldsymbol{n} + \boldsymbol{j}_q + \alpha_q(T - T_a) + (1 - \varepsilon)\alpha_m\lambda(W - W_a) = 0 \text{ on } S_2 \tag{4}$$

$$W = W_a \text{ on } S_3 \tag{5}$$

$$k_m \nabla W\boldsymbol{n} + \boldsymbol{j}_m + k_m\delta\nabla T\boldsymbol{n} + \alpha_m(W - W_a) = 0 \text{ on } S_4 \tag{6}$$

$$S_1 \cup S_2 = \partial R \tag{7}$$

$$S_3 \cup S_4 = \partial R \tag{8}$$

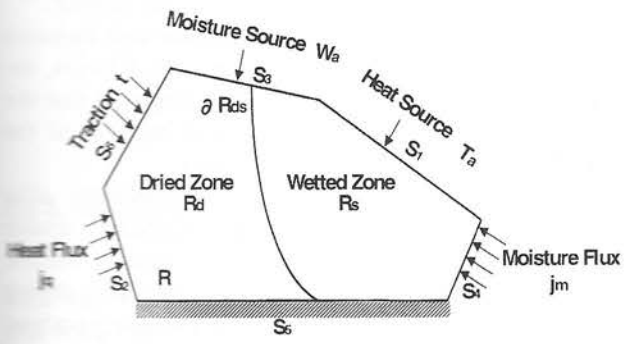

Fig. 1. Mechanical modeling of the drying process and structural behaviour of ceramic electric insulators.

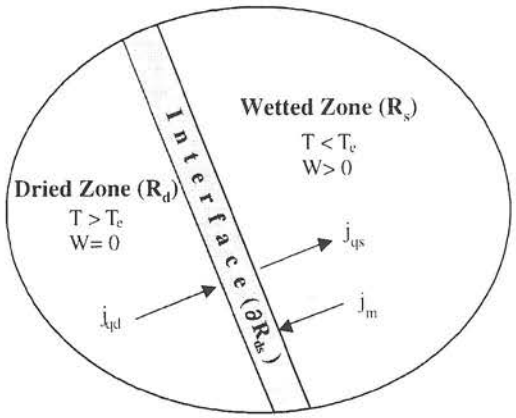

Fig. 2. Schematic view of heat and moisture transfer in the interface.

where T_a is a prescribed temperature on the boundary S_1, $\boldsymbol{j}_q$ is heat flux on the boundary S_2, W_a is a prescribed moisture on the boundary S_3, $\boldsymbol{j}_m$ is moisture flux on the boundary S_4, k_q is a thermal conductivity, k_m is moisture conductivity, $\boldsymbol{n}$ is a outward normal vector on the surface of the boundary, α_q is a convective heat transfer coefficient, α_m is a convective moisture transfer coefficient, ε is a ratio of the vapour diffusion coefficient to the total diffusion coefficient of moisture, λ is a heat of phase change, δ is a thermo-gradient coefficient, and ∂R is a boundary of control volume R. Eq. (3) and eq. (5) represent boundary conditions on the portion of the material boundary where constant temperature and constant moisture are prescribed, respectively.

At the evaporation temperature during the heat and moisture transfer, a phase change phenomenon that the moisture within the material is liquefied or evaporized happens and there exists two phases simultaneously. In order to efficiently analyze the heat and moisture transfer during phase change process, the effect of a latent heat is considered. Energy conservation in the interface between the dried zone and the wetted zone can be written as follows (see Fig. 2):

$$L(W_0\dot{\boldsymbol{X}} + \boldsymbol{j}_m) \cdot \boldsymbol{n}_{ds} = (\boldsymbol{j}_{qd} - \boldsymbol{j}_{qs}) \cdot n_{ds} \tag{9}$$

where L is a latent heat of evaporation, W_0 is a resident moisture content, $\boldsymbol{X}$ is a position of interface, $\boldsymbol{n}_{ds}$ is a unit normal vector in phase change zone, $\boldsymbol{j}_{qd}$ is a heat flux vector in dried zone, and $\boldsymbol{j}_{qs}$ is a heat flux vector in wetted zone.

Structural Analysis

The governing equation in stress field can be expressed as follows:

$$\nabla \cdot \boldsymbol{\sigma} + \boldsymbol{f} = 0 \tag{10}$$

where $\boldsymbol{\sigma}$ is a stress tensor and $\boldsymbol{f}$ is a body force vector.

Also, the boundary conditions can be described as follows:

$$\boldsymbol{u} = \boldsymbol{u}_a \text{ on } S_5 \tag{11}$$

$$\boldsymbol{\sigma} \cdot \boldsymbol{n} = \boldsymbol{t} \text{ on } S_6 \tag{12}$$

where $\boldsymbol{u_a}$ is a prescribed displacement on the boundary S_5 and $\boldsymbol{t}$ is a traction on the boundary S_6.

The basic assumption in a constitutive model in stress field is that a strain tensor represents the sum of the strains caused by traction, temperature, and moisture:

$$e = \frac{1}{E}(\sigma - \sigma_0) + \alpha\Delta T + \beta\Delta W \tag{13}$$

where e is a total strain tensor, σ is a stress tensor, σ_0 is an initial stress tensor, α is a thermal expansion coefficient, ΔT is a temperature gradient, β is a moisture expansion coefficient, and ΔW is a moisture gradient. An elastic coefficient matrix, $[E]$, is evaluated as follows:

$$[E] = \frac{E(1-\nu)}{(1+\nu)(1-2\nu)} \begin{bmatrix} 1 & \frac{\nu}{1-\nu} & \frac{\nu}{1-\nu} & 0 \\ & 1 & \frac{\nu}{1-\nu} & 0 \\ & & 1 & 0 \\ & \text{sym.} & & \frac{1-2\nu}{2(1-\nu)} \end{bmatrix} \tag{14}$$

In the finite element formulation of hygro-thermal stress problem, the thermal and moisture effects may be treated as that of an initial stress.

The constitutive equation can be defined as follows:

$$\sigma = E \cdot (e - \alpha\Delta T - \beta\Delta W) + \sigma_0 = E \cdot e + \sigma'_0 \tag{15}$$

Following the standard finite element procedure, we can finally have

$$\sum_{e=1}^{E} ([K]\{u\} - \{F\})_e = 0 \tag{16}$$

where,

$$[K] = \int_R [B_u]^* E [B_u] dR \tag{17}$$

$$\{F\} = \int_{\partial\Omega} [N_u] t dR + \int_R [N_u] f dR - \int_R [B_u]^* \sigma'_0 dR \tag{18}$$

In eq. (17) and eq. (18), is defined as follows:

$$[B_u]^* = \begin{bmatrix} \frac{1}{r} + \frac{\partial}{\partial r} & 0 & -\frac{1}{r} & \frac{\partial}{\partial z} \\ 0 & \frac{\partial}{\partial z} & 0 & \frac{1}{r} + \frac{\partial}{\partial r} \end{bmatrix} \tag{19}$$

Numerical Examples

In order to check the compatibility of a current design of ceramic electric insulators, the drying process is simulated and the structural analysis is performed.

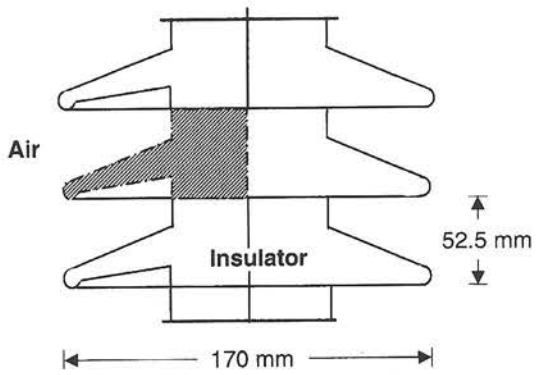

Fig. 3. Schematic view of a ceramic electric insulator for a drying analysis.

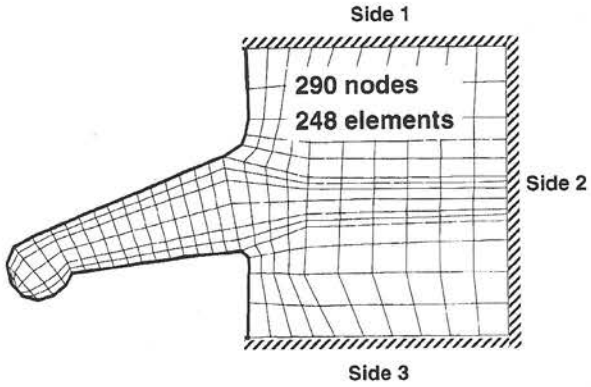

Fig. 4. Finite element model of a ceramic electric insulator for a drying analysis.

Drying Analysis

A schematic view of a ceramic electric insulator is illustrated in Fig. 3. The hatched area is modeled for the simulation due to the symmetry. Figure 4 shows finite element model. Finite element mesh consists of 290 nodes and 248 quadrilateral linear elements. The green insulator initially lies in a constant temperature 25°C and moisture 80 kg/m^3 state. The ambient temperature and moisture are 60°C and 40 kg/m^3, respectively. Adiabatic and symmetric conditions are imposed on three sides except the boundary exposed to the air. The material properties of ceramic electric insulator are listed in Keum *et al.* [15] As the time elapses, the heat and moisture transfer from the boundary to the interior.

Figure 5 and Fig. 6 show temperature and moisture distributions after drying for 1 hour and 5 hours, respectively. As the time goes on, it is supposed that the hygro-thermal stress should be bigger because of the big temperature and moisture gradients.

Figure 7 shows principal stress distributions after drying for 1 hour and 5 hours. The maximum tensile principal stress occurs at the corner of ceramic electric insulator. Maximum tensile principal stress after drying for 1 hour is 40.7 MN/m^2. Maximum tensile principal stress after drying for 5 hours is 174.0 MN/m^2.

Figure 8 shows deformed shapes after drying for 1

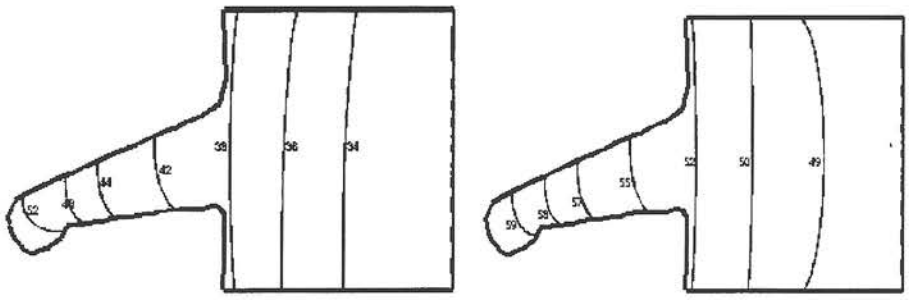

Fig. 5. Temperature distribution of ceramic electric insulator after drying.

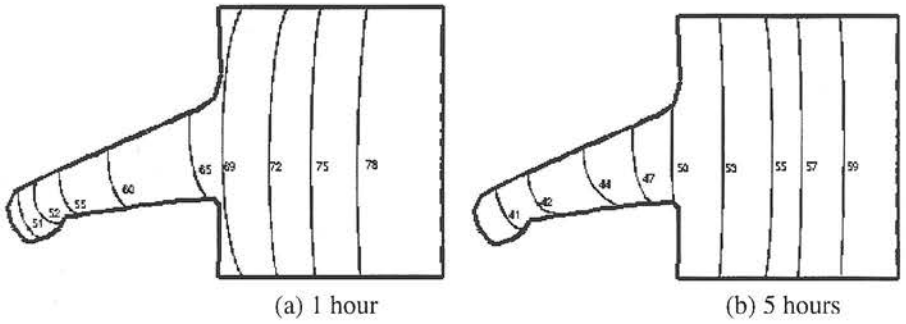

Fig. 6. Moisture distribution of ceramic electric insulator after drying.

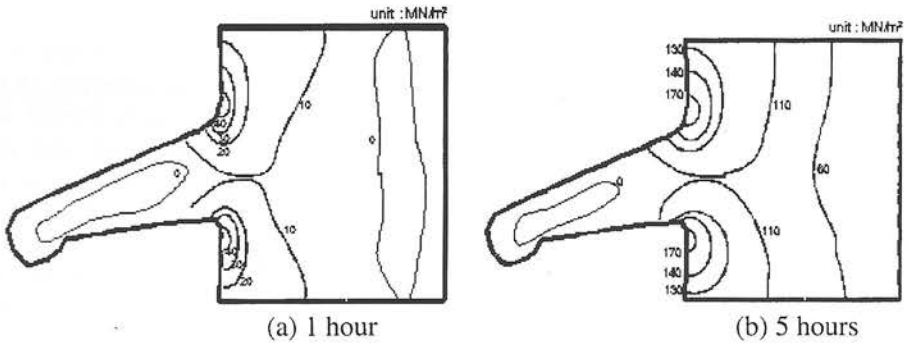

Fig. 7. Principal stress distribution of ceramic electric insulator after drying.

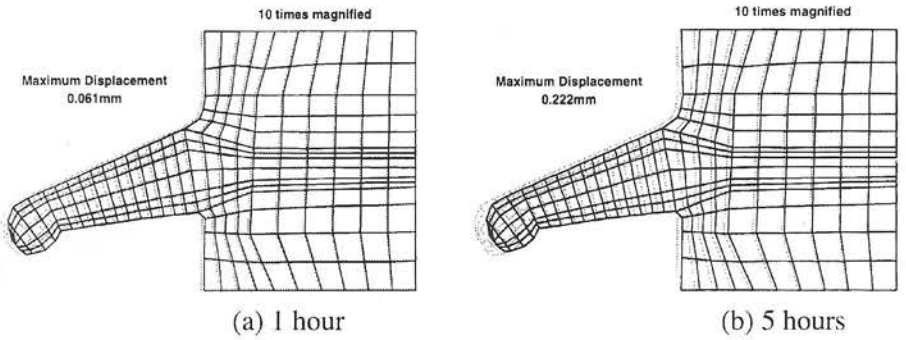

Fig. 8. Deformed shape of ceramic electric insulator after drying.

hour and 5 hours. Dotted line stands for initial shape and solid line means deformed shape. Maximum displacements are 0.061 mm and 0.222 mm at the edge of the wing after 1 hour and 5 hours, respectively.

Structural Analysis

A schematic view of a ceramic electric insulator for a structural analysis is illustrated in Fig. 9. Due to the symmetry, the half of the axial section is modeled. The

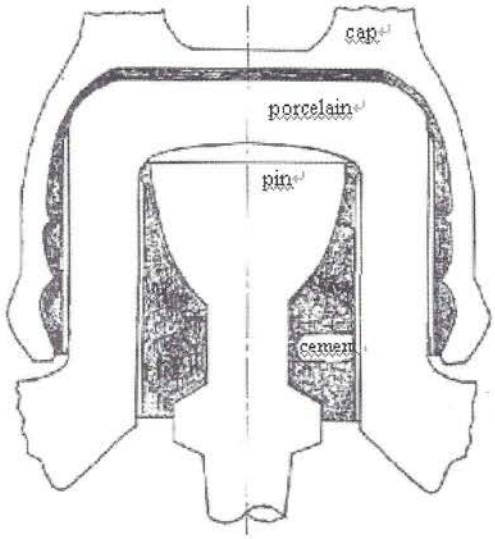

Fig. 9. Schematic view of a ceramic electric insulator for a structural analysis.

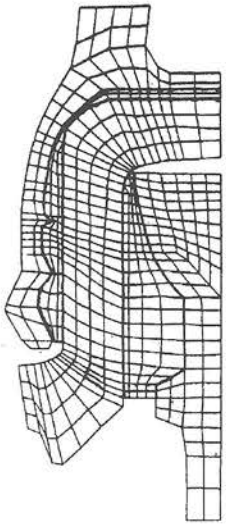

Fig. 10. Finite element model of a ceramic electric insulator for a structural analysis.

finite element mesh for a structural analysis, which consists of 628 nodes and 511 axi-symmetric quadrilateral elements, is shown in Fig. 10.

Two boundary conditions are imposed: One is a natural boundary condition in the bottom of the pin. The other is an essential boundary condition in the top of the cap.

Figure 11 shows the principal stress distribution in an interior of the electric insulator. The tension is acted on the pin and cap of the insulator. The porcelain and cement transfer the tension and transform it into the compression. The bending force in the lower part of the porcelain is applied by the resistance force of the pin. It helps the crack diffusion in the cap lip. Though the cap jaw and cap lip are mainly loaded by the tension, the cap head is affected by the bending.

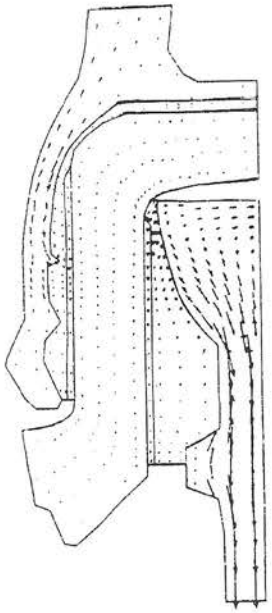

Fig. 11. Principal stress distribution in an insulator interior.

Redesign

Based on the drying and structural analyses, the guidelines of precise design of ceramic insulators are prepared as follows:

(1) The strength of the electric insulator is affected by the shape, size, and position of the pin. If the pin size is improper, the large tension load is occurred in the inner part of porcelain and then it accelerates tension fracture in the cap lip. As a result, the strength of the insulator is decreased.

(2) The strength of the insulator is affected by the position and the number of the cap jaw, but independent on the pin geometry. When the direction of the tension in the cap jaw and that of the tension in the

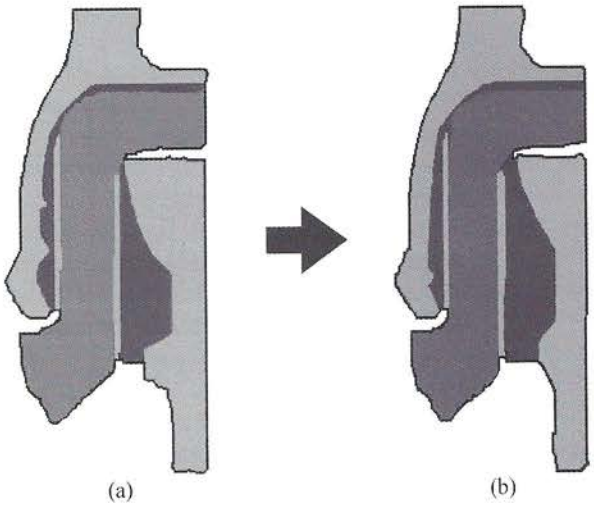

Fig. 12. (a) Original shape and (b) redesigned shape of ceramic electric insulator.

upper of the pin are coincided, a crack is initiated.

(3) At the corner where there are sudden changes in geometry, the maximum stress is concentrated such that the minimization of the differences in temperature and moisture between ambient air and green ceramics is needed.

Using the guidelines, the redesign of the electric insulator was performed as shown in Fig. 12 and it was verified through experiments that failing load is increased about 25% of that of the original design.

Conclusions

The finite element simulations to propose the guidelines of precise design of ceramic insulators and to see the compatibility of a current design of the insulator are carried out. Through this study, the following conclusions are derived:

(1) Finite element formulation in temperature-moisture and stress fields is derived.

(2) The drying analysis considering heat and moisture movements and the structural analysis considering electric cable weight are carried out.

(3) The design guidelines based on the finite element simulations are prepared.

(4) The new geometry of the ceramic electric insulator is proposed for an optimal design.

Acknowledgements

This work was supported by the Korea Science and Engineering Foundation (KOSEF) through the Ceramic Processing Research Center at Hanyang University.

References

1. A.V. Luikov, "Systems of Differential Equations of Heat and Mass Transfer in Capillary-Porous Bodies (Review)", Int. J. Heat Mass Transfer, Vol. 18, pp. 1-14, 1975.
2. A.V. Luikov, Heat and Mass Transfer in Capillary Porous Bodies, Pergamon, Oxford, 1975.
3. A.V. Luikov, Heat, and Mass Transfer, Mir Publishers, Moscow, 1980.
4. S. Whitaker, "Simultaneous Heat, Mass and Momentum Transfer in Porous Media: A Theory of Drying", Advances in Heat Transf. 13 (1977) 119-203.
5. D.A. De Vris, "Simultaneous Transfer of Heat and Moisture in Porous Media", Trans. Am. Geophys. Un. 39[5] (1958) 909-916.
6. J.R. Philip, and D.A. De Vris, "Moisture Movement In Porous Materials under Temperature Gradients", Trans. Am. Geophys. Un. 38[2] (1957) 222-232.
7. G. Comini, and R.W. Lewis, "A Numerical Solution of Two-Dimensional Problem Involving Heat and Mass Transfer", Int. J. Heat Mass Transfer 19 (1976) 1387-1392.
8. H.R. Thomas, R.W. Lewis, and K. Morgan, "An Application of The Finite Element Method to The Drying of Timber", Wood Fibre, 11 (1980) 237-243.
9. G. Dhatt, M. Jacquemier, and C. Kadje, "Modelling of Drying Refractory Concrete", Drying '86, [1] (1986) 94-104.
10. Z.X. Gong, and A.S. Mujumdar, "Development of Drying Schedules for One-Heating Drying Refractory Concrete Slabs Based on A Finite Element Model", J. Am. Ceram. Soc. 79[6] (1969) 1649-1658.
11. R.W. Lewis, M. Strada, and G. Comini, "Drying-Induced Stressed in Porous Bodies", Int. J. Num. Meth. Engng. 11 (1977) 1175-1184.
12. G.C. Sih, A. Ogawa, and S.C. Chou, "Two-Dimensional Transient Hygrothermal Stresses in Bodies with Circular Cavities : Moisture and Temperature Coupling Effects", J. Thermal Stresses 4 (1981) 193-222.
13. A.H. Heuer, Finite Element Analysis of a Ceramic Cone Insulator, American Ceramic Society Bulletin, 54[6] (1975).
14. Takayuki Iwama, and Kunizi Kito, Ultra-high Strength Suspension Insulators and Insulator String Assemblies for UHV Transmission Line, IEEE PAS-101, 1982.
15. Y.T. Keum, J.H. Jeong, and K.H. Auh, Finite Element Simulation of Ceramic Drying Processes, Modeling and Simulation in Material Science and Engineering, 8[4] (2000) 541-556.